25 New Light Curves and Updated Ephemeris through Analysis of Exoplanet WASP-50 b with EXOTIC

Ramy Mizrachi
Stanford Online High School, 415 Broadway Academy Hall, Floor 2, 8853, Redwood City, CA 94063; ramymizrachi@gmail.com

Dylan Ly
Stanford Online High School, 415 Broadway Academy Hall, Floor 2, 8853, Redwood City, CA 94063; wuyifighter@gmail.com

Leon Bewersdorff
Citizen Scientist, Sandkaulbach 3-5, 52062 Aachen, North Rhine-Westphalia, Germany; leon.bewersdorff@rwth-aachen.de

Kalée Tock
Stanford Online High School, 415 Broadway Academy Hall, Floor 2, 8853, Redwood City, CA 94063; kaleeg@stanford.edu

Received July 21, 2021; revised August 2, 29, September 24, 2021; accepted September 24, 2021

Abstract EXOplanet Transit Interpretation Code (EXOTIC) was used to reduce 75 sets of time-series images of WASP-50 taken by the 6-inch telescope of the Center for Astrophysics | Harvard & Smithsonian MicroObservatory. Of these sets, 25 resulted in clean light curves showing the transit of WASP-50 b, 22 of which had sufficiently low uncertainty to qualify for use in an ephemeris update. We used these results to establish planetary parameters and update WASP-50 b's mid-transit time from 2455558.61237 ± 0.0002 to 2456295.68245 ± 0.00085 (BJD_TDB) and its period from 1.9551 ± 5^{-06} to 1.95509584 ± 0.00000106 d. The mid-transit time uncertainty of WASP-50 b at the time of projected James Webb Telescope science operations (January 2022) is reduced by a factor of 4.0 using our new ephemeris. We also calculate the planetary size and semi-major axis of WASP-50 b to be approximately 83,200 km ± 2,230 km and 0.0294 AU ± 0.0000233 AU, respectively.

1. Introduction

The search for planets outside our solar system has historically been possible with expensive space telescopes. However, even a smaller optical telescope can detect a reduction in the light of a star due to a transiting exoplanet if the host star is bright enough, and if the planet itself is large enough relative to its host. The shorter the period of the orbit, the more often the exoplanet can be observed, thereby preventing the accumulation of uncertainty in transit mid-time. Also, the reduced light curve from each transit can be used to better characterize both the orbit and properties of the planet. Therefore, as citizen scientists make more observations, space telescopes and large ground-based telescopes are able to spend less valuable observation time observing transits whose timing is uncertain.

For a planet with close proximity to the host star, the orbital period is typically on the order of a few days. Since 2001, the Center for Astrophysics | Harvard & Smithsonian MicroObservatory has hosted a campaign to collect images of such large, short-period exoplanets (Sadler *et al.* 2001). Over 75 sets of time-series images of WASP-50 b's transit have accumulated in their archives. The gas giant slightly exceeds the mass of Jupiter at 1.468 Jupiter masses, and it orbits a G-type star. It is a characteristic hot-Jupiter with a short period of around 1.9 days and an orbital radius of 0.0294 AU, or about 3 percent the distance from the Earth to the Sun (Gillon *et al.* 2011).

2. Observations

MicroObservatory hosts a network of automated remote three-foot-tall reflecting telescopes, each with a 6-inch mirror, 560-mm focal length, and KAF1400 CCD with 9-micron pixels. With 2 × 2 binning, the image size is 650 × 500 pixels at a pixel scale of 5"/px. MicroObservatory takes images of several exoplanet systems and makes the past month's images publicly available for educational use via their website, at

https://mo-www.cfa.harvard.edu/MicroObservatory/

(Sadler *et al.* 2001).

3. Weather

MicroObservatory uses weather data from NOAA IR satellite images for the region available when the images were taken. The software marks the location where the telescope is, encircles it, and then remaps the pixels within the circle from their 8-bit scale to a 0 to 100 relative scale. The value 0 signifies a complete overcast, whereas a value of 100 would signify that the sky is perfectly clear.

The other metric used by MicroObservatory to determine uncertainty on transits is delta temperature. This metric gives the absolute value difference between the CCD detector and a sensor at the telescope optical tube. Cooled detectors provide a better signal-to-noise ratio because they have less dark current. Dark current is a source of noise from free electrons in the camera sensor arising from thermal energy. To reduce this source of noise, the difference in temperature from the MicroObservatory's ambient temperature should be at least 10° C (Sienkiewicz 2021).

Due to changes in the weather during a transit, some of the images within a transit series might be usable, even if images from other parts of the series are obscured. When this occurs, as it did with the 2013-10-27 transit, it is not possible to fit a

reliable light curve that includes all the datapoints. A plot of the weather quality and delta temperature for the 2013-10-27 transit is shown in Figure 1. Unstable seeing indicates poor images, as is shown towards the end of the graph, and an unstable temperature can indicate both a potential change in mechanical focus and efficiency of dark subtraction, as these both depend on a stable temperature.

The final images of the transit are obscured due to weather and have a significantly brighter sky background. Images with a large half-width half maximum were also removed as shown in Figure 2. We chose to remove further outlier images during the transit event that deviated by more than 3 median average distances (MAD) from the surrounding 20 datapoints using HOPS (HOlomon Photometric Software) version 3.0 (Tsiarias 2019).

An image of the original 2013-10-27 light curve is shown in Figure 3. A transit is clearly visible in the initial part of the image sequence, but the poor image quality at the end does not allow for an accurate fit.

The light curve in Figure 4 shows the 2013-10-27 transit after removing the low-quality images. Visually, this is a much better fit. Also, EXOTIC shows the residuals on the bottom sub-plot and reports a "scatter in the residuals" parameter. This parameter is the standard deviation of the residuals in units of percent (relative to baseline flux), which can easily be compared to the transit depth. Once the low-quality images are removed from the 2013-10-27 series, the scatter in the residuals drops from 7.78% to 0.7%, and the mid-transit time shifts from 2456592.927 ± 0.003 d to 2456592.8586 ± 0.0051 d.

Although there is a slight increase in mid-transit uncertainty, it is still under our threshold of 0.007 on mid-transit uncertainty, and is deemed more accurate than the mid-time resulting from the fit shown in Figure 3. This demonstrates the importance of verifying the quality of the observational data themselves, and not solely relying on low fit errors. The process thus produces another usable light curve for WASP-50 b, which would not have been taken into consideration for O–C and ephemeris calculation otherwise, based on the initial review of the image data.

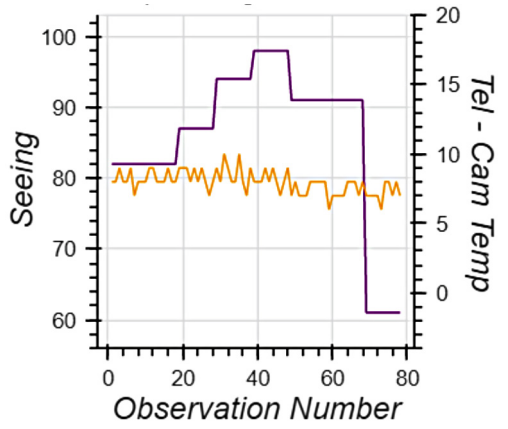

Figure 1. Observation Quality for 2013-10-27 transit. Seeing: avg 86, std 11. Temp diff: avg 8.0, std 0.8. The purple line represents seeing conditions (left axis) and the yellow line represents the ambient temperature in the telescope tube minus the temperature of the CCD detector (right axis).

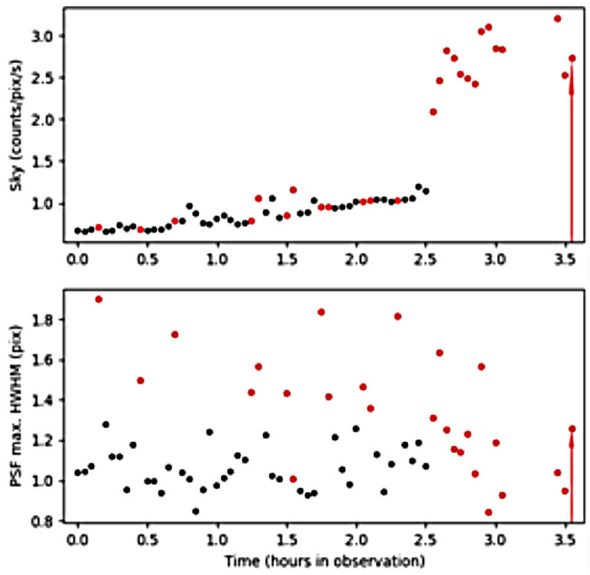

Figure 2. Red points represent outliers removed using HOPS.

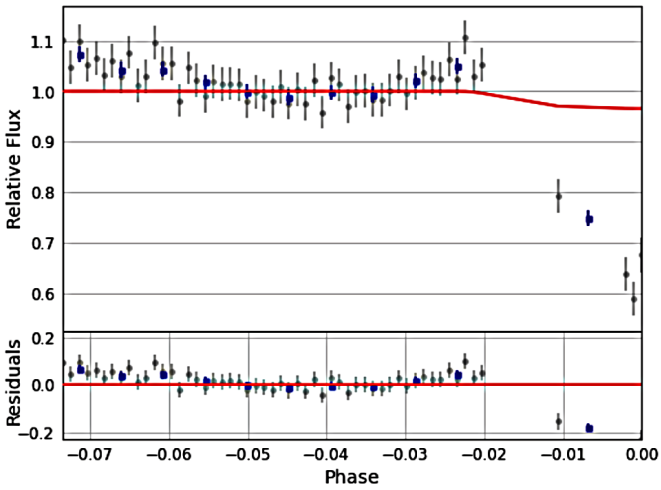

Figure 3. 2013-10-27 light curve with red line showing the fit before removal of outliers.

4. Data reduction and photometry

For the photometric evaluation of the data, Exoplanet Watch's EXOTIC (EXOplanet Transit Interpretation Code) software was chosen (Zellem *et al.* 2020). This software requires the user to select up to ten comparison stars (comp stars). Comparison stars AUD 000-BMD-470 and AUD 000-BMD-471 were selected based on the American Association of Variable Star Observers (AAVSO) Variable Star Plotter (VSP; AAVSO 2021), shown in Figure 5. The AAVSO chart ID X26441FB can be entered on the AAVSO VSP website for retrieval. Apart from giving EXOTIC the option to choose from the two AAVSO-recommended comparison stars, we chose three additional comp star candidates, which are labeled in Figure 6 as C3, C4, and C5, to provide more options for EXOTIC's reduction of our light curves. The manually selected comparison stars were all bright, close to the target, and not too close to other stars in the field.

EXOTIC was created by Exoplanet Watch, a citizen science initiative of NASA Jet Propulsion Laboratory. Its purposes

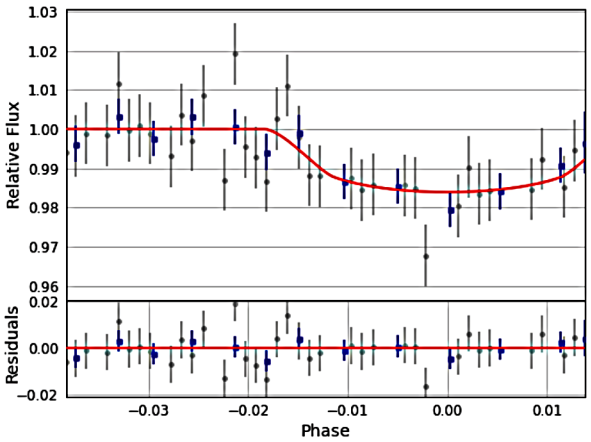

Figure 4. 2013-10-27 light curve after removing outliers.

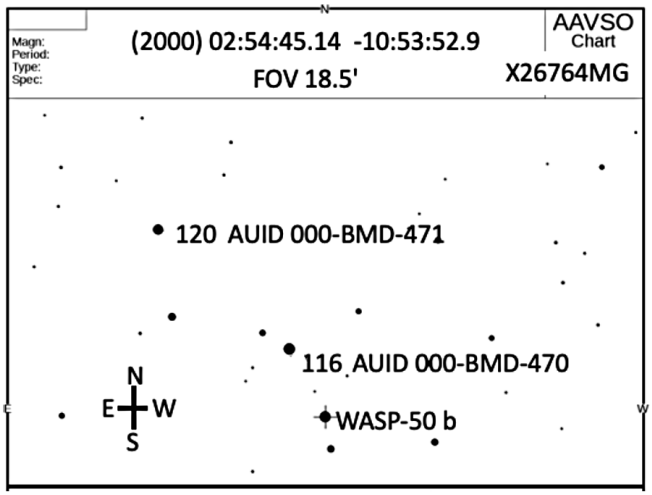

Figure 5. AAVSO VSP view of WASP-50 starfield.

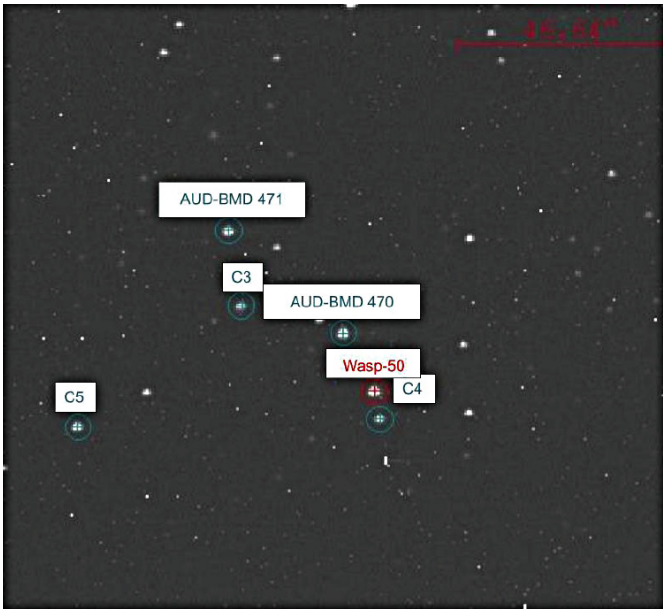

Figure 6. WASP-50 labeled starfield with manually selected extra comps in AstroImageJ (Collins *et al.* 2017).

are both to introduce citizen scientists into astronomy, and to reduce uncertainty of exoplanet transit midpoints in preparation for coming NASA missions, such as the James Webb Space Telescope. EXOTIC can be run locally or by using Google Colaboratory (Colab). We used Colab so that team members could share files and to avoid using local computer resources or space allocation. The script mounts the user's Google Drive account and installs EXOTIC onto a virtual machine in the cloud. It then displays the first image of the series and prompts the user for the target name, the coordinates the target, and up to ten comparison stars. The target name is used to look up parameters in the NASA Exoplanet Archive (NEA) to use as priors in the light curve fit. Then EXOTIC aligns the images and determines the optimal inner and outer photometric apertures. The inner aperture encompasses the star's point spread function (PSF) without including the sky background, which fills the space between the outer and inner apertures. EXOTIC determines the optimal aperture sizes by fitting to a Gaussian PSF model (Fatahi 2021). To account for changes in sky brightness affecting the measured flux, EXOTIC subtracts the background photon count from the star's flux. Finally, the change in flux of the target star is compared to the light emitted by each of the selected comparison stars, and a "quick fit" is performed. The comparison star with the best quick fit is selected for use in the more rigorous fitting routine. For these images, EXOTIC selected one of the AAVSO VSP-recommended comp stars over the manually identified options in 21 of 22 light curve fits, which confirms its agreement with the VSP-recommended stars.

EXOTIC's output included a light curve for each series along with the scatter in the residuals, the midpoint time, transit depth, transit duration, semi-major axis relative to the stellar radius, and planetary versus stellar radius (Winn 2014).

5. Data

EXOTIC's reduction process produced 25 new light curves of WASP-50 b, which are shown in Appendix A. Each plot shows the measured normalized flux with error bars of the host star versus time as the exoplanet transits across its face along with the best possible light curve fit. EXOTIC also outputs planetary radius/stellar radius, transit depth, and semi-major axis over stellar radius. These parameters were all averaged and an uncertainty is reported for these parameters as the standard error of the mean (SEM), or the standard deviation of each parameter divided by the square root of the number of data points. The transit depth is therefore 0.020 ± 0.10, the planetary radius over stellar radius is 0.142 ± 0.00380, and the semi-major axis over stellar radius is 7.49 ± 0.0418. We calculate WASP-50 b to have a radius 14.2% the size of WASP-50, a G-type main sequence star (Gillon *et al.* 2011). From the ratio of the planet to the stellar radius (R_p/R_s) the planetary size can be determined. The literature value of 0.843 solar radii (5.870×10^5 km) for WASP-50 (Chakrabarty and Sengupta 2019) is used for R_s to calculate the radius of the planet in km:

$$r_{km} = R_s * (R_p/R_s) \pm SEM \quad (1)$$

The orbital distance in Astronomical Units (AU) can also be determined from the ratio between the semi-major axis and the star radius (a/R_s). A planet with a larger semi-major axis thus has a longer transit, which EXOTIC takes into account when fitting this parameter to an individual light curve:

$$d_{AU} = \frac{R_s * (a/R_s)}{1.496 * 10^8 \text{ km}} * 1\text{AU} \pm \frac{\text{SEM}}{1.496 * 10^8 \text{ km}} * 1\text{AU} \quad (2)$$

These two calculations and their respective SEM calculation are performed for each transit reduced with EXOTIC. The results are reported in AU to align with the units used in the literature.

Here the planetary size of WASP-50 b is calculated to be approximately 83200km ± 2230 km or 1.190 ± 0.032 R_J. The same is done for the semi-major axis, which is calculated to be 0.0294AU ± 0.0000233 AU. The planetary size and semi-major axis are within the uncertainty of those presented in the literature of 1.15 ± 0.05 R_J and 0.0295 ± 0.0009 AU, respectively (Gillon *et al.* 2011).

The transit mid-times from the MicroObservatory transits calculated using EXOTIC are shown in Table 1.

We produced an O–C plot for WASP-50 b using the 22 bolded epochs from Table 1, for which the scatter in the residuals was less than 1.6% and the mid-transit time uncertainty was less than 0.007 day. Using the most recently published values, t_0 = 2455558.61237 BJD (Bonomo *et al.* 2017) and p = 1.9551 d (Chakrabarty and Sengupta 2019), our data produced the plot shown in Figure 7:

The ephemeris of an exoplanet allows times of transit-minima to be calculated. This calculation includes information about the period of the planet, the transit mid-times, and the uncertainties of measurements. Using image sets of WASP-50 b transits, we were able to update the ephemeris using EXOTIC. The orbital ephemeris of WASP-50 b is modeled using the following equation:

$$t_{next} = n * P + T_{mid} \quad (3)$$

where t_{next} is a future mid-transit time, P is the period, n is the orbital epoch, and T_{mid} is a reference mid- transit time. The linear ephemeris is optimized using nested sampling to derive posterior distributions for the mid-time and period. (Pearson 2019). The code uses the epochs, mid-transit times, and mid-transit uncertainties for each of the 22 transits and bounds for the mid-transit time and period. The output includes graphs depicting the uncertainties as well as values for the mid-transit time and period. The most recent listing in the NASA Exoplanet Archive cites 1.955100 ± 0.000005 d as the period (Chakrabarty and Sengupta 2019) and 2455558.61237 ± 0.00020 BJD_TDB as the mid-transit time (Bonomo *et al.* 2017). Based on the ephemeris fitter's analysis of our transits, the updated period and mid-transit time are 1.95509584 ± 0.00000106 d and 2456295.68245 ± 0.00085 d, respectively.

$$t_{next} = n * 1.95509584 + 2456295.68245 \quad (4)$$

Equation 4 represents our proposed new ephemeris. The graphs for the linear ephemeris fit and the residuals versus

Table 1. Transit midtimes for WASP-50b from MOBs data.

Transit Number	*Date*	*Epoch*	*Mid-transit (BJD_TDB) (2450000+)*	*Mid-transit Uncertainty (days)*	*Scatter (%)*
1	2013-01-03	377	6295.6795	0.0016	0.85
2	2013-09-14	507	6549.8496	0.0029	1.08
3	2013-10-27	529	6592.8618	0.004	0.62
4	2013-10-31	531	6596.7662	0.0025	0.65
5	2013-11-02	532	6598.7236	0.0027	0.74
6	2013-12-13	553	6639.7807	0.0022	0.82
7	2013-12-15	554	6641.7389	0.0018	1.11
8	2014-11-22	729	6983.8763	0.0033	0.78
9	2014-11-26	731	6987.7864	0.0022	0.76
10	2014-11-30	733	6991.6938	0.0027	0.78
11	2015-12-28	934	7384.6742	0.0029	0.96
12	*2016-12-04*	*1109*	*7726.817*	*0.026*	*1.22*
13	2017-11-15	1286	8072.8631	0.0025	0.79
14	2017-11-17	1287	8074.814	0.0019	0.69
15	2018-01-03	1311	8121.734	0.0037	1.23
16	2018-01-05	1312	8123.6972	0.0022	0.73
17	*2018-09-14*	*1441*	*8375.898*	*0.029*	*1.11*
18	*2018-11-04*	*1467*	*8426.77*	*0.076*	*1.12*
19	2018-11-06	1468	8428.6902	0.0022	0.95
20	2018-12-21	1491	8473.6535	0.0032	1.42
21	2019-10-14	1643	8770.8366	0.0031	1.25
22	2020-09-24	1820	9116.8825	0.0045	1.13
23	2020-09-26	1821	9118.856	0.0032	1.1
24	2020-11-12	1845	9165.767	0.003	0.87
25	2020-12-25	1867	9208.776	0.0022	1.11

Note: Italicized transits are not used in the O–C plot.

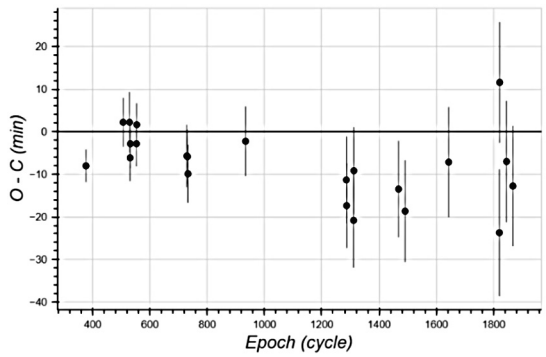

Figure 7. O–C plot for WASP-50 b using t_0 = 2455558.61237 and p = 1.9551.

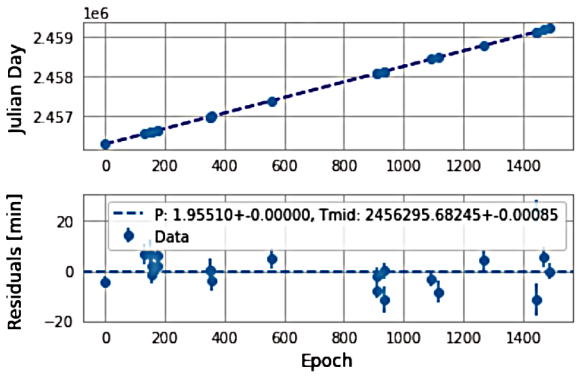

Figure 8. Graph of linear ephemeris fit from ephemeris updater code and graph of residuals against epoch.

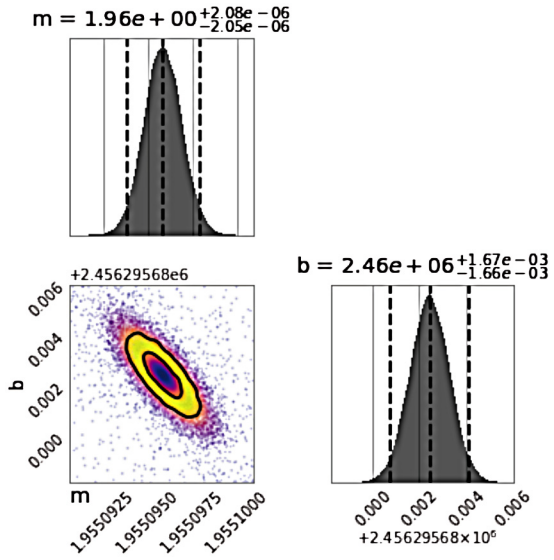

Figure 9. Posterior distributions of the updated mid-transit time and period.

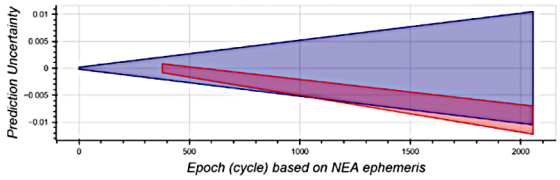

Figure 10. Cone plot comparing our mid-transit prediction (red) to the current NEA prediction (blue) for 1 January 2022. Previous and new ephemerides superimposed with prediction difference offset.

epochs are shown in Figure 8, and the posterior distributions of the mid-transit time and period are shown in Figure 9.

6. Results

The utility of the new ephemeris can be evaluated by playing forward the prediction to 2022-01-01, which is when the James Webb Space Telescope is projected be ready to commence science operations. In Figure 10, the NEA prediction (blue) is compared to our prediction (pink) on that date. As is evident from the figure, our analysis has caused WASP-50 b's mid-transit time uncertainty on 2022-01-01 to decrease by a factor of 4.0 relative to the previous NEA prediction. Our new midpoint prediction for 2022-01-01 is 2459580.24346 ± 0.00262, which is –13.8 minutes different from the NEA prediction of 2459580.25307 ± 0.01049.

7. Conclusion

We present 25 new mid-time values and light curves for WASP-50 b from the MicroObservatory observations and established parameters for WASP-50 b's size and orbit, supporting its classification as a hot Jupiter-type exoplanet. We used the result of the light curve reduction to establish planetary parameters and update the mid-transit time from 2455558.61237 ± 0.0002 to 2456295.68245 ± 0.00085 (BJD_TDB) and the period from 1.9551 ± 5^{-6} to 1.95509584 ± 0.00000106 d (Gillon *et al.* 2011). Based on the 22 sets of time-series images taken by the 6-inch MicroObservatory telescope, the uncertainty of the predicted midpoint in January of 2022 has decreased by a factor of 4.0.

8. Future work

With at least five additional light curves and mid-time values, it would be possible to search for TTVs (Transit Timing Variations), which might constitute the signature of another planet in the WASP-50 system.

9. Acknowledgements

Data used here come from the MicroObservatory telescope archives maintained by Frank Sienkiewicz, who also provides information on weather and delta temperature measurements. MicroObservatory is maintained and operated as an educational service by the Center for Astrophysics | Harvard & Smithsonian and is a project of NASA's Universe of Learning, supported by NASA Award NNX16AC65A. Additional MicroObservatory sponsors include the National Science Foundation, NASA, the Arthur Vining Davis Foundations, Harvard University, and the Smithsonian Institution.

Thanks to Martin Fowler for his advice and help with analysis of these data, and to Rob Zellem and his team for fixing and maintaining the EXOTIC software. Also, thanks to Jason Eastman for creating the public time conversion calculator on the "astroutils" website.

This research has made use of the NASA Exoplanet Archive, which is operated by the California Institute of Technology, under contract with the National Aeronautics and Space Administration under the Exoplanet Exploration Program.

This publication makes use of the EXOTIC data reduction package from Exoplanet Watch, a citizen science project managed by NASA's Jet Propulsion Laboratory on behalf of NASA's Universe of Learning. This work is supported by NASA under award number NNX16AC65A to the Space Telescope Science Institute.

References

AAVSO. 2021, Variable Star Plotter (VSP; https://www.aavso.org/apps/vsp/).
Bonomo, A. S., *et al.* 2017, *Astron. Astrophys.*, **602A**, 107.
Chakrabarty, A., and Sengupta, S. 2019, *Astron. J.*, **158**, 39.
Collins, K. A., Kielkopf, J. F., Stassun1, K. G., and Hessman, F. V. 2017, *Astron. J.*, **153**, 77 (https://www.astro.louisville.edu/software/astroimagej)
Fahati, T. 2021, private communication (September 13, 2021).
Gillon, M. *et al.* 2011, *Astron. Astrophys.*, **533A**, 88.
Pearson, K. A. 2019, *Astron. J.*, **158**, 243.
Sadler P., *et al.* 2001, *J. Sci. Education Technol.*, **10**, 39.
Sienkiewicz, F. 2021, private communication (March 25, 2021).
Tsiaras, A. 2019, in *EPSC-DPS Joint Meeting 2019*, id. EPSC-DPS2019-1594.
Winn, J. N. 2014, arXiv:1001.2010v5.
Zellem R., *et al.* 2020, *Publ. Astron. Soc. Pacific*, **132**, 054401.

Appendix A: Light curves of WASP-50 b reduced with EXOTIC